

## Fast Synthesis, Formation Mechanism, and Control of Shell Thickness of CuS Hollow Spheres

Haitao Zhu,<sup>\*,†,‡</sup> Jixin Wang,<sup>†,‡</sup> and Daxiong Wu<sup>†</sup>

<sup>†</sup>College of Materials Science and Engineering, Qingdao University of Science and Technology, Qingdao 266042, P. R. China., and <sup>‡</sup>State Key Laboratory Breeding Base of Photocatalysis, Fuzhou University, Fuzhou 350002, P. R. China

Received February 1, 2009

CuS hollow spheres were quickly synthesized under mild conditions with spherical aggregates of Cu<sub>2</sub>O nanoparticles as sacrificial templates. The mechanism involved in the synthesis process has been studied using transmission electron microscopy, high-resolution transmission electron microscopy, scanning electron microscopy, X-ray diffraction, thermal gravimetry, and Fourier transform infrared spectra. The results show that the formation of loose aggregates of Cu<sub>2</sub>O nanoparticles is the key to the fast synthesis of hollow spheres at low temperature. The thickness of the shell can be controlled easily by adjusting the aggregation degree of the Cu<sub>2</sub>O nanoparticles.

### 1. Introduction

Hollow spheres have attracted considerable attention because of their unique properties and widespread applications in drug delivery, catalysis, sensors, artificial cells, and photonic crystals, and so on.<sup>1–6</sup> Various fabrication procedures for hollow structures have been developed, such as hard templates, soft templates, as well as physical/chemical processes based on the Kirkendall effect, Ostwald ripening, chemically induced self-transformation, and so on.<sup>7–14</sup> Among them, the sacrificial template chemical transformation method based on the Kirkendall effect has been

demonstrated to be an effective approach.<sup>11,15–25</sup> In this method, the sacrificial templates transform to the aimed at shell through chemical reaction on the templates' surface, and the core is removed by Kirkendall diffusion at the same time, and therefore no modification of the template surface and no special process for removing the template core are needed. The method also has the advantages of low cost and materials saving. However, because effective diffusion only takes place at higher temperature, high temperature and/or long time (several to tens of hours under hydrothermal or annealing condition<sup>15,19–21</sup>) are needed to obtain hollow microspheres by completely removing the core templates. Is it possible to synthesize hollow microspheres quickly using this method under mild condition? In addition, the core template completely transforms to the aimed at shell by chemical reaction, that is, the thickness of the sphere shell is mainly determined by the amount of effective reactants supplied by the relevant sacrificial template. How can the shell thickness of hollow spheres be controlled in this method?

As an important semiconductor with unique electronic, optical, and chemical properties, copper monosulfide (CuS) is a promising material with potential application in many

\*To whom correspondence should be addressed. E-mail: htzhu1970@163.com. Phone: +86 532 84022676. Fax: +86 532 84022787.

- (1) Caruso, F. *Adv. Mater.* **2001**, *13*, 11.
- (2) Kim, S. W.; Kim, M.; Lee, W. Y.; Hyeon, T. *J. Am. Chem. Soc.* **2002**, *124*, 7642.
- (3) Park, S.; Lim, J. H.; Chung, S. W.; Mirkin, C. A. *Science* **2004**, *303*, 348.
- (4) Grosso, D.; Boissiere, C.; Sanchez, C. *Nat. Mater.* **2007**, *6*, 572.
- (5) Maji, T. K.; Matsuda, R.; Kitagawa, S. *Nat. Mater.* **2007**, *6*, 142.
- (6) Sander, M. S.; Cote, M. J.; Gu, W.; Kile, B. M.; Tripp, C. P. *Adv. Mater.* **2004**, *16*, 2052.
- (7) Caruso, F.; Caruso, R. A.; Mohwald, H. *Science* **1998**, *282*, 1111.
- (8) Qi, L.; Li, J.; Ma, J. *Adv. Mater.* **2002**, *14*, 300.
- (9) Peng, Q.; Dong, Y.; Li, Y. *Angew. Chem., Int. Ed.* **2003**, *42*, 3027.
- (10) Sun, Y.; Xia, Y. *Science* **2002**, *298*, 2176.
- (11) Yin, Y.; Rioux, R. M.; Erdonmez, C. K.; Hughes, S.; Somorjai, G. A.; Alivisatos, A. P. *Science* **2004**, *304*, 711.
- (12) Zeng, H. C. *J. Mater. Chem.* **2006**, *16*, 649.
- (13) Yu, J.; Guo, H.; Davis, S. A.; Mann, S. *Adv. Funct. Mater.* **2006**, *16*, 2035.
- (14) Liu, J.; Xue, D. *Adv. Mater.* **2008**, *20*, 2622.
- (15) Liu, B.; Zeng, H. C. *J. Am. Chem. Soc.* **2004**, *126*, 16744.
- (16) Cao, H. L.; Qian, X. F.; Wang, C.; Ma, X. D.; Yin, J.; Zhu, Z. K. *J. Am. Chem. Soc.* **2005**, *127*, 16024.
- (17) Yin, Y. D.; Erdonmez, C. K.; Cabot, A.; Hughes, S.; Alivisatos, A. P. *Adv. Funct. Mater.* **2006**, *16*, 1389.
- (18) Tan, H.; Li, S. P.; Fan, W. Y. *J. Phys. Chem. B* **2006**, *110*, 15812.

- (19) Fan, H. J.; Gosele, U.; Zacharias, M. *Small* **2007**, *3*, 1660.
- (20) Kim, M. R.; Jang, D. J. *Chem. Commun.* **2008**, 5218.
- (21) Cabot, A.; Smith, R. K.; Yin, Y. D.; Zheng, H. M.; Reinhard, B. M.; Liu, H. T.; Alivisatos, A. P. *ACS Nano* **2008**, *2*, 1452.
- (22) Qiu, Y. F.; Yang, S. H. *Nanotechnology* **2008**, *19*, 265606.
- (23) Yang, Y.; Kim, D. S.; Scholz, R.; Knez, M.; Lee, S. M.; Gosele, U.; Zacharias, M. *Chem. Mater.* **2008**, *20*, 3487.
- (24) Nakamura, R.; Tokozakura, D.; Nakajima, H.; Lee, J. G.; Mori, H. *J. Appl. Phys.* **2007**, *101*, 74303.
- (25) Wang, C. G.; Xu, Z. D.; Liu, R. *Chem. Res. Chinese U.* **2008**, *24*, 249.

fields, such as a sensor, solar radiation absorber, catalyst, and nanometer-scale switch, and so on.<sup>26–29</sup> At present, several methods, such as solvothermal-microwave, solvothermal, hydrothermal, chemical conversion, and sonication methods,<sup>30–42</sup> have been used to synthesize CuS hollow spheres. For example, Xie's and Qian's group prepared CuS hollow spheres under hydrothermal condition at 160–180 °C for 12–24 h.<sup>34–43</sup> Zhu et al. developed a thioglycolic acid assisted hydrothermal process to synthesize submicrometer-sized CuS hollow spheres at 200 °C for 20 h.<sup>41</sup> Using sulfur liquid droplets as template, Wan et al. synthesized CuS hollow spheres through interfacial reaction of CuCl with sulfur liquid droplets at 125 °C for 2 days.<sup>42</sup> With 2-hydroxypropyl- $\beta$ -cyclodextrin as template, Xu et al. fabricated CuS hollow spheres under sonication.<sup>40</sup> Thongtem prepared CuS hollow spheres using a solvothermal-microwave process.<sup>30</sup> Recently, Gao reported the synthesis of thick-shell and thin-shell CuS hollow spheres using CuBr solid spheres or spherical aggregates (consisting of the Cu<sup>+</sup>, Br<sup>-</sup>, and (C<sub>4</sub>H<sub>9</sub>)<sub>4</sub>N<sup>+</sup> ions) as the sacrificial templates under hydrothermal treatment at 160 °C.<sup>32</sup> These two kinds of templates were prepared by different reactants and processes; hence it is difficult to control the shell thickness by using one kind of template. Although much progress has been made in the synthesis of CuS hollow spheres, it remains a major challenge to develop a fast and mild route to the preparation of hollow structures with controllable shell thickness.

Herein, a rapid and mild solution method is reported for the preparation of CuS hollow spheres via the chemical transformation of in situ formed Cu<sub>2</sub>O spheres as sacrificial templates. The Cu<sub>2</sub>O spheres are loose aggregates of Cu<sub>2</sub>O nanoparticles. The mechanism shows that the formation of loose aggregates of Cu<sub>2</sub>O nanoparticles is the key to the fast synthesis of hollow spheres at low temperature. The thickness of the shell can be controlled easily by adjusting the aggregation degree of the Cu<sub>2</sub>O nanoparticles.

## 2. Experimental Section

All reagents were of analytical grade and used without further purification. Twenty-five milliliters of 2 mmol·L<sup>-1</sup> CuSO<sub>4</sub> solution (0.05 mmol CuSO<sub>4</sub>) and 0.24 g of poly(vinylpyrrolidone) (PVP-K30) were added into a conical flask under magnetic stirring at room temperature. Then, 25 mL of NaOH solution with pH value of 9.0 (prepared by dropping 0.01 mol·L<sup>-1</sup> fresh NaOH solution into distilled water until the pH value of the mixture reached 9.0) was added into the above mixture. After being stirred for 2 min, 2.0 mL of 0.10 mol·L<sup>-1</sup> N<sub>2</sub>H<sub>4</sub>·H<sub>2</sub>O solution was added. A suspension of Cu<sub>2</sub>O spheres was obtained after a reaction of 5 min. Then 0.266 mmol thioacetamide was added into the above suspension, and the temperature of the mixture was heated to 40 °C. After a further reaction of 1 h at 40 °C under magnetic stirring, the product was obtained, centrifuged, washed with distilled water and ethanol, and then dried under vacuum at room temperature. By repeating the experiment for 10 times, the total product yields of Cu<sub>2</sub>O and CuS spheres were about 82% and 76%, respectively. To investigate the formation mechanism, interim samples were collected after adding thioacetamide, and were characterized. Because thioacetamide is a CMR (carcinogen, mutagen, and toxic to reproduction) compound, it is important to wash the hands and exposed skin carefully after its handling.

The pH value of NaOH solution was measured using a Sartorius PB-10 acid-meter. The Powder X-ray diffraction (XRD) analyses data were recorded on a Rigaku D/Max r-A diffractometer. The scanning electron microscopy (SEM) images were taken with FESEM-6700 field-emission microscope. The transmission electron microscopy (TEM) images and the selected area electron diffraction (SAED) were captured on a JEM-2000EX transmission electron microscope. The high-resolution transmission electron microscopy (HRTEM) was performed on a JEM-2010 transmission electron microscope. Fourier transform infrared (FT-IR) spectra were recorded on a Nicolet 510P FT-IR Spectrometer using KBr pellet technique in the range of 400–4000 cm<sup>-1</sup>. Thermal gravimetric (TG) analysis was carried out on a TG209F apparatus at a heating rate of 4 °C·min<sup>-1</sup> from 25 to 800 °C under air atmosphere. The photoluminescence (PL) measurement was performed on an F-4500 FL spectrophotometer at room temperature. The X-ray photoelectron spectroscopy (XPS) experiments were carried out on a Thermo Escalab 250 system using Al K $\alpha$  radiation. The samples used for XPS analysis were washed with distilled water and ethanol three times, respectively, and then dried under dynamic vacuum at 100 °C for 4 h.

## 3. Results and Discussions

**3.1. Characterization of Cu<sub>2</sub>O Templates.** Figure 1a shows the XRD pattern of the Cu<sub>2</sub>O templates. All diffraction peaks in the pattern can be indexed to the pure cubic phase of Cu<sub>2</sub>O with lattice constant  $a = 4.258 \text{ \AA}$  (JCPD file No. 77-0199). The average crystalline size was calculated to be 11 nm according to the Debye–Scherrer formula. Figure 2a is the SEM image of Cu<sub>2</sub>O templates, showing that the as-prepared Cu<sub>2</sub>O nanoparticles are regular spheres. The size distribution of the Cu<sub>2</sub>O spheres was estimated from SEM images analysis of at least 300 particles. The size distribution of Cu<sub>2</sub>O spheres (Figure 2d) shows that it is nearly monodispersed with main size of 220 nm. The SEM image of high magnification (inset in Figure 2a) indicates that the spheres are made up of Cu<sub>2</sub>O nanoparticles. The TEM image (Figure 2b), HRTEM image (Figure 2c), and SAED (inset in Figure 2b) of an individual sphere show that

- (26) Zhang, X. J.; Wang, G. F.; Gu, A. X.; Wei, Y.; Fang, B. *Chem. Commun.* **2008**, 5945.  
 (27) Yuan, K. D.; Wu, J. J.; Liu, M. L.; Zhang, L. L.; Xu, F. F.; Chen, L. D.; Huang, F. Q. *Appl. Phys. Lett.* **2008**, *93*, 132106.  
 (28) Raevskaya, A. E.; Stroyuk, A. L.; Kuchmii, S. Y.; Kryukov, A. I. *J. Mol. Catal. A: Chem.* **2004**, *212*, 259.  
 (29) Sakamoto, T.; Sunamura, H.; Kawaura, H.; Hasegawa, T.; Nakayama, T.; Aono, M. *Appl. Phys. Lett.* **2003**, *82*, 3032.  
 (30) Thongtem, T.; Phuruangrat, A.; Thongtem, S. *Curr. Appl. Phys.* **2009**, *9*, 195.  
 (31) Zhu, Y. F.; Fan, D. H.; Shen, W. Z. *Langmuir* **2008**, *24*, 11131.  
 (32) Gao, J. N.; Li, Q. S.; Zhao, H. B.; Li, L. S.; Liu, C. L.; Gong, Q. H.; Qi, L. M. *Chem. Mater.* **2008**, *20*, 6263.  
 (33) Nan, Z. D.; Wei, C. Z.; Wang, X. Y.; Hao, H. Y. *Chin. J. Chem.* **2008**, *26*, 1395.  
 (34) Li, B. X.; Xie, Y.; Xue, Y. J. *Phys. Chem. C* **2007**, *111*, 12181.  
 (35) He, Y. J.; Yu, X. Y.; Zhao, X. L. *Mater. Lett.* **2007**, *61*, 3014.  
 (36) Yu, X. L.; Cao, C. B.; Zhu, H. S.; Li, Q. S.; Liu, C. L.; Gong, Q. H. *Adv. Funct. Mater.* **2007**, *17*, 1397.  
 (37) Ni, Y. H.; Liu, R.; Cao, X. F.; Wei, X. W.; Hong, H. M. *Mater. Lett.* **2007**, *61*, 1986.  
 (38) Deng, H.; Chen, C.; Peng, Q.; Li, Y. D. *Mater. Chem. Phys.* **2006**, *100*, 224.  
 (39) Xu, H. L.; Wang, W. Z.; Zhu, W.; Zhou, L. *Nanotechnology* **2006**, *17*, 3649.  
 (40) Xu, J. Z.; Xu, S.; Geng, J.; Li, G. X.; Zhu, J. J. *Ultrason. Sonochem.* **2006**, *13*, 451.  
 (41) Zhu, H. L.; Ji, X.; Yang, D.; Ji, Y. J.; Zhang, H. *Microporous Mesoporous Mater.* **2005**, *80*, 153.  
 (42) Wan, S. M.; Guo, F.; Shi, L.; Peng, Y. Y.; Liu, X. Z.; Zhang, Y. G.; Qian, Y. T. *J. Mater. Chem.* **2004**, *14*, 2489.  
 (43) Chen, X. Y.; Wang, Z. H.; Wang, X.; Zhang, R.; Liu, X. Y.; Lin, W. J.; Qian, Y. T. *J. Cryst. Growth* **2004**, *263*, 570.

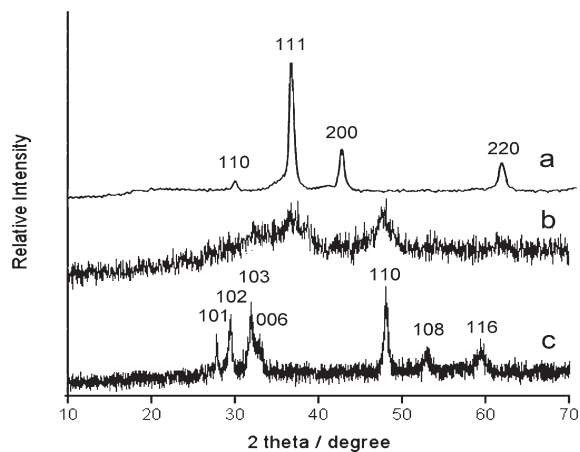


**Figure 1.** XRD patterns of (a)  $\text{Cu}_2\text{O}$  spheres, (b) intermediate product that reacted with thioacetamide for 10 min, and (c)  $\text{CuS}$  hollow spheres.

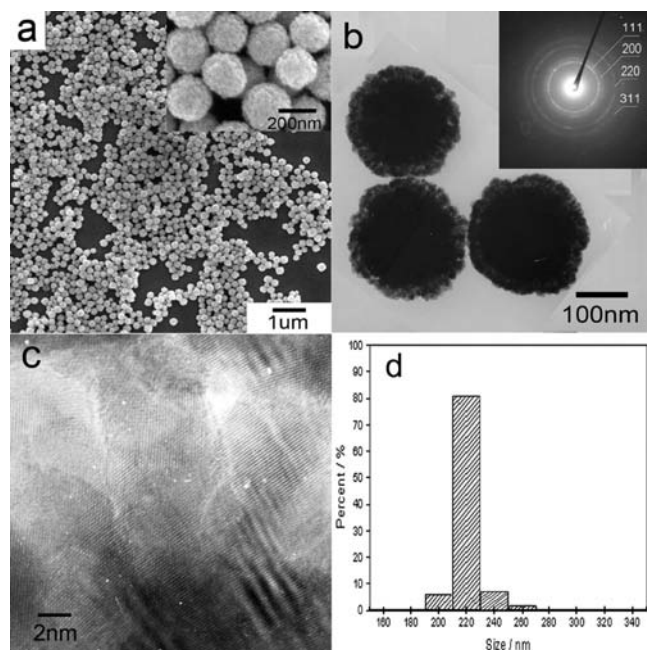
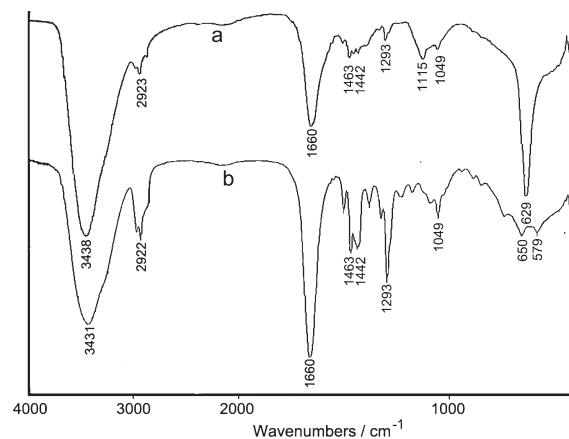


**Figure 2.** Characterization of  $\text{Cu}_2\text{O}$  spheres: (a) SEM image, (b) TEM image and SAED pattern of an individual  $\text{Cu}_2\text{O}$  sphere, (c) HRTEM image, and (d) size distribution. Inset of (a) is the high magnification image of  $\text{Cu}_2\text{O}$  spheres. The size data was collected by about 300  $\text{Cu}_2\text{O}$  spheres from SEM and TEM photos.

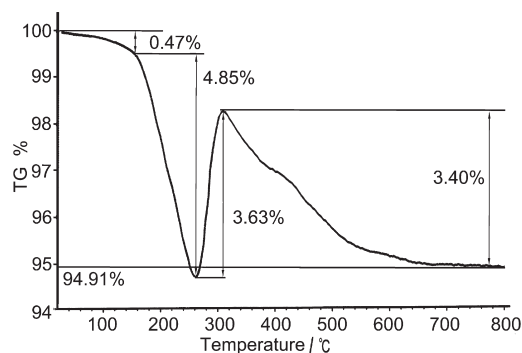
the  $\text{Cu}_2\text{O}$  spheres are loose aggregates of  $\text{Cu}_2\text{O}$  nanoparticles, and the size of nanoparticles is about 10–15 nm.

Figure 3 is the FT-IR spectra of the as-fabricated  $\text{Cu}_2\text{O}$  spheres and pure PVP. The absorption bands at 2922, 1660, 1463, 1442, 1292, and 1049  $\text{cm}^{-1}$  can be assigned to the PVP molecules. The peak at 3431  $\text{cm}^{-1}$  is corresponded to the stretching mode of the hydroxyls of adsorbed water. According to the Standard IR spectra of  $\text{Cu}_2\text{O}$  and  $\text{CuO}$  (SADTLER file No.Y1171K and Y1170K, respectively), the peak at 629  $\text{cm}^{-1}$  is attributed to the  $\text{Cu}-\text{O}$  vibration of the  $\text{Cu}_2\text{O}$  nanocrystals. It is clear that the as-prepared  $\text{Cu}_2\text{O}$  sphere is composed of  $\text{Cu}_2\text{O}$  nanoparticles and PVP molecules.

The XPS spectra of  $\text{Cu}_2\text{O}$  spheres are shown in the Supporting Information, Figure S1. The O 1s peak can be



**Figure 3.** FT-IR spectra of the  $\text{Cu}_2\text{O}$  spheres (a) and pure PVP (b).



**Figure 4.** TG curve of obtained  $\text{Cu}_2\text{O}$  spheres.

fitted into 4 peaks. The main peak at 530.2 eV is indexed to  $\text{O}^{2-}$  in  $\text{Cu}_2\text{O}$ .<sup>44</sup> Other peaks at 531.2, 531.6, and 529.5 eV are assigned to the O in PVP,  $-\text{OH}$ , and  $\text{CuO}$ , respectively.<sup>44,45</sup> The  $\text{Cu } 2p_{3/2}$  fitted peak reveals a main peak at 932.2 eV, corresponding to  $\text{Cu}^+$  in  $\text{Cu}_2\text{O}$ .<sup>46</sup> The presence of a weak satellite feature on the higher binding energy side indicates the presence of a small amount of  $\text{CuO}$ .<sup>44</sup> According to the XRD pattern (Figure 1a), the formed product is pure  $\text{Cu}_2\text{O}$ . Therefore, it is deduced that a small fraction of surface  $\text{Cu}_2\text{O}$  was oxidized to  $\text{CuO}$  during the samples' drying and handling under normal ambient conditions.<sup>44,47</sup>

The TG curve of the  $\text{Cu}_2\text{O}$  spheres (Figure 4) shows both weight losses and gains. The first weight loss (up to 150  $^{\circ}\text{C}$ , 0.47%) is due to the removal of adsorbed water molecules, and the second one (150–260  $^{\circ}\text{C}$ , 4.85%) should be attributed to the decomposition of a part of PVP. In the next step, a weight increase of 3.63% (260–310  $^{\circ}\text{C}$ ) corresponds to the oxidation of  $\text{Cu}_2\text{O}$ . In fact, during this period a weight loss and a weight increase happen simultaneously, but the weight increase is larger than the weight loss. Above 310  $^{\circ}\text{C}$ , decomposition of the residual PVP leads to a further weight loss. After being heated to 760  $^{\circ}\text{C}$ , the residue is  $\text{CuO}$ , which is 94.91% of the weight of the original sample. According to the transformation reaction from  $\text{Cu}_2\text{O}$  to  $\text{CuO}$ , there should

(45) Beamson, G.; Briggs, D. *High Resolution XPS of Organic Polymers: the Scienta ESCA300 Database*; Wiley Interscience: New York, 1992.

(46) Nakai, I.; Sugitani, Y.; Nagashima, K.; Niwa, Y. *J. Inorg. Nucl. Chem.* **1978**, *40*, 789.

(47) Yin, M.; Wu, C. K.; Lou, Y. B.; Burda, C.; Koberstein, J. T.; Zhu, Y. M.; O'Brien, S. *J. Am. Chem. Soc.* **2005**, *127*, 9506.

be a theoretical weight increase of 9.55% (the amount of  $\text{Cu}_2\text{O}$  is 85.36%). Thus, from 260 to 310 °C the net weight loss would be 5.92% (9.55–3.63%). In the range from 160 to 760 °C, there is a total weight loss of (4.85% + 5.92% + 3.40%) 14.17%, corresponding to the decomposition of the PVP.

From the above results, it is clear that the  $\text{Cu}_2\text{O}$  spheres are loose aggregates of 85.36%  $\text{Cu}_2\text{O}$  nanoparticles and 14.17% PVP molecules. According to our previous work, the formation of the loose aggregates is due to modification and steric effect of the PVP molecules.<sup>48</sup>

**3.2. Characterization of CuS Hollow Spheres.** Using the obtained  $\text{Cu}_2\text{O}$  spheres as sacrificial templates, CuS hollow spheres were synthesized by sulfidation reaction in the mother solution at 40 °C. Figure 1c shows the XRD pattern of the obtained product. It can be seen that all peaks in the pattern can be indexed to hexagonal covellite CuS with lattice constants  $a = 3.792 \text{ \AA}$ ,  $b = 16.34 \text{ \AA}$  (JCPD file No. 06-0464). The average crystalline size was calculated to be 12.5 nm using the Debye–Scherrer formula. The TEM image of the as-prepared sample is shown in Figure 5a. The contrast between the dark edge and the pale center evidence the hollow structure. The size distribution (Figure 5d) derived from TEM images analysis shows that the CuS hollow spheres are nearly monodispersed. The outer diameter (OD), inner diameter (ID), and shell thickness of CuS hollow spheres are 280 nm, 200 nm, and 40 nm, respectively. Compared with the size of precursor  $\text{Cu}_2\text{O}$  spheres (220 nm, Figure 2d), the change of size is related to the formation mechanism of these CuS hollow spheres (as discussed below). The SAED pattern (Figure 5b) and HRTEM image (Figure 5c) of the shell show that it consists of CuS nanoparticles. The lattice spacing of 2.7 Å corresponds well to the {0 0 6} planes of the hexagonal CuS.

Figure 5e is the SEM image of the CuS hollow spheres. Some small nanoparticles can be seen on the spheres' surface, making it rough. In the SEM observation, no broken hollow spheres were found. After ultrasonic crushing for 30 min (20 kHz, 250 w), only a few broken spheres were found (Figure 5g). The energy-dispersed X-ray (EDX) analysis result is shown in Figure 5g. The strong peaks for Cu and S can be found in the spectrum. It reveals that the molar ratio of Cu to S is 29.6:30.3, which is close to the stoichiometry of CuS. The Si peak came from the silicon substrate used to support the samples.

The XPS spectra of CuS hollow spheres are shown in the Supporting Information, Figure S2. The O 1s peak can be fitted into 2 peaks. The peaks at 531.2 and 531.6 eV are indexed to O in PVP and –OH, respectively.<sup>44,45</sup> The two peaks located at 932.5 and 952.3 eV are assigned to Cu 2p in CuS, and the two peaks at 161.9 and 163.2 eV correspond to S 2p in CuS.<sup>49,50</sup> The ratio of integral area for Cu 2p to S 2p is about 1: 1.078. The XPS results show that the obtained CuS is stoichiometric, which is in good agreement with the result of EDX.

TG analysis of the CuS hollow spheres (Supporting Information, Figure S3) also shows both weight losses

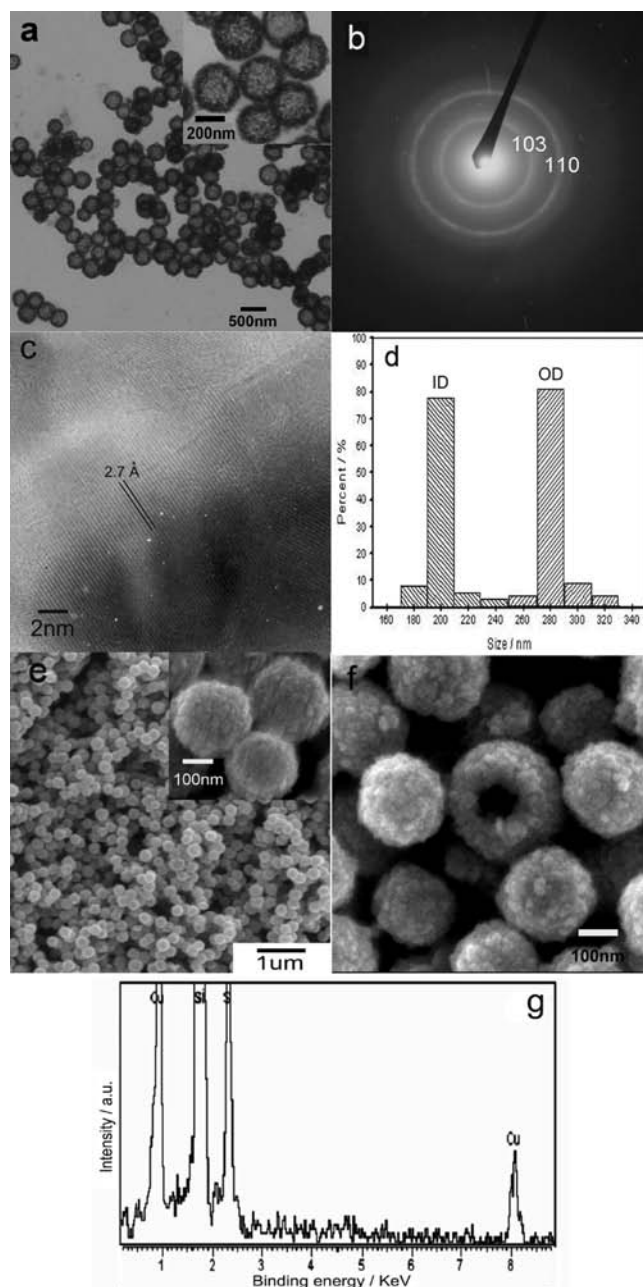


**Figure 5.** Characterization of CuS hollow spheres: (a) TEM image, (b) SAED of an individual CuS sphere, (c) HRTEM image of shell, (d) size distribution, (e) SEM image of obtained CuS hollow spheres, (f) SEM image of CuS hollow spheres crushed for 30 min under ultrasonication, (g) EDX spectra. The insets in panels a and e are the high magnification TEM and SEM image of CuS hollow spheres, respectively. The size data was collected by about 300 CuS spheres from SEM and TEM images.

and gains. The first weight loss (up to 150 °C, 0.93%) is due to the removal of absorbed water molecules, and the second one (150–330 °C, 18.13%) should be attributed to the decomposition of a part of PVP and transformation from CuS to  $\text{Cu}_{1.8}\text{S}$  and  $\text{Cu}_2\text{S}$ .<sup>50,51</sup> In the next step, a weight increase of 31.87% (330–580 °C) corresponds to the formation of  $\text{CuO} \cdot \text{CuSO}_4$  and  $\text{CuSO}_4$ .<sup>50,51</sup> Above 580 °C, the decomposition of  $\text{CuO} \cdot \text{CuSO}_4$  and  $\text{CuSO}_4$  leads to a further weight loss (33.75%).<sup>50,51</sup> After being heated to 760 °C, 78.06% of the original weight is

(48) Zhu, H. T.; Wang, J. X.; Xu, G. Y. *Cryst. Growth Des.* **2009**, *9*, 633.

(49) Zhang, Y. C.; Qiao, T.; Hu, X. Y.; Zhou, W. D. *Mater. Res. Bull.* **2005**, *40*, 1696.

(50) Wu, C.; Yu, S. H.; Chen, S.; Liu, G.; Liu, B. *J. Mater. Chem.* **2006**, *16*, 3326.

(51) Dunn, J. G.; Muzenda, C. *Thermochim. Acta* **2001**, *369*, 117.

left for the final product CuO.<sup>50,51</sup> According to the transformation reaction from CuS to CuO, the weight of CuS in the hollow spheres is 93.76%. Thus, the weight of PVP in the hollow spheres is 5.31%.

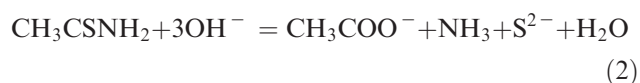
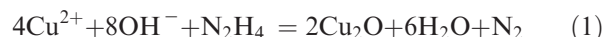
The PL spectrum of the CuS hollow spheres shows a sharp excitonic emission at 370 nm (Supporting Information, Figure S4). These polycrystalline hollow spheres are composed of nanometer-sized CuS crystals. There may be surface defects and an interface coupling effect between the grain boundaries, resulting in an increase of the wave function overlap, which contributes to a narrower energy gap. The sharp excitonic emission indicates that the CuS hollow spheres are of high optical quality.

### 3.3. Formation Mechanism of the CuS Hollow Spheres.

To study the transformation process from Cu<sub>2</sub>O spheres to hollow CuS spheres, samples collected at different reaction times (5 min, 10 min, and 15 min after adding thioacetamide into the Cu<sub>2</sub>O suspension) were characterized via the TEM, SAED, and XRD analysis. The Cu<sub>2</sub>O spheres, which served as sacrificial template, are about 220 nm in diameter (Figure 2d). After thioacetamide was added into the Cu<sub>2</sub>O suspension, S<sup>2-</sup> released from the decomposition of thioacetamide reacts with the Cu<sub>2</sub>O nanoparticles on the spheres' surface to produce CuS nanoparticles. At a reaction time of 5 min, some grayish CuS nanoparticles are produced surrounding the dark

Cu<sub>2</sub>O spheres (Figure 6a). A core–shell structure with a small gap is formed at 10 min (Figure 6b). However, the shell is non-uniform. Some holes are found to exist in the thin wall (as the arrows show in Figure 6b). The average diameter of the core–shell spheres is about 240 nm. The XRD pattern of this sample (Figure 1b) and the SAED of an individual sphere (Figure 6c) indicate the coexistence of Cu<sub>2</sub>O and CuS nanoparticles. Uniform and dense shells are formed at 15 min (Figure 6d). The core still exists, but the gap between core and shell broadens. The average diameter of core–shell spheres is about 250 nm. When the reaction time is 1 h, the core–shell spheres completely transform to hollow CuS spheres with average outer diameter and inner diameter of about 280 and 200 nm, respectively (Figure 5d).

On the basis of the experimental results, the following reactions may be involved:



The formation mechanism of a hollow sphere is proposed and illustrated in Figure 7. In the first step, S<sup>2-</sup> reacts with the Cu<sub>2</sub>O nanoparticles on the Cu<sub>2</sub>O spheres' surface to produce CuS nanoparticles surrounding the Cu<sub>2</sub>O spheres. With the further reaction, a non-uniform shell of CuS nanoparticles is formed surrounding the Cu<sub>2</sub>O core. The CuS shell separates the inner Cu<sub>2</sub>O nanoparticles with the outer sulfur ion and prevents further direct chemical reaction between the two reactants. Therefore, there will be concentration gradient of copper ion and sulfur ion from the solution outside the CuS shell to the surface of the Cu<sub>2</sub>O spheres inside the shell. Under the driving force of the concentration gradient, the sulfur ions in the solution will diffuse inward through the CuS shell to its inside surface while the copper ions will diffuse outward through the CuS shell to its outside. Then CuS nanoparticles are formed on the outside and inside surfaces of the CuS shell. The holes in the shell become a shortcut for mass diffusion and transferance; the production rate of CuS in these locations is high, and the thickness of the shell increases rapidly. As a result, uniform and dense shells are formed. Because the diffusion velocity of copper ions is faster than that of sulfur ions in the CuS shell,<sup>39</sup> which is named as the Kirkendall effect, the production of CuS on the outside of the shell is

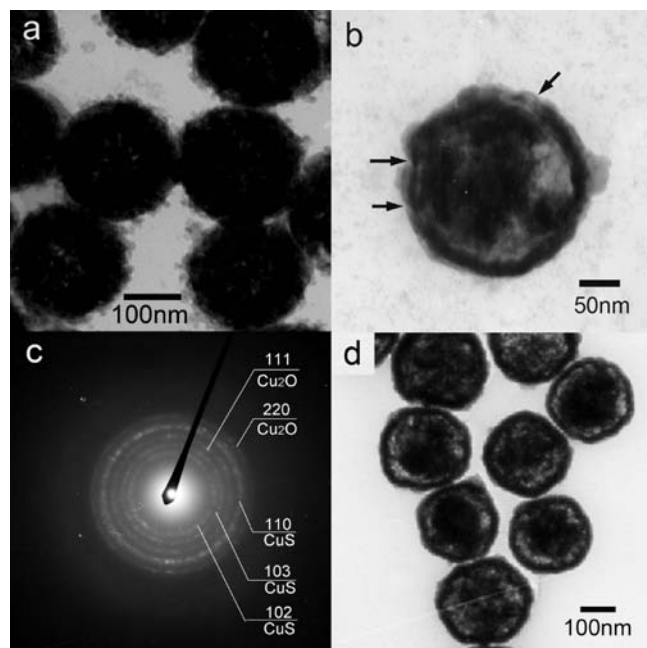


**Figure 6.** TEM images (a, b, d) and SAED (c) pattern of samples collected at different reaction times after thioacetamide adding into the Cu<sub>2</sub>O suspension. (a) 5 min, (b) and (c) 10 min, (d) 15 min.

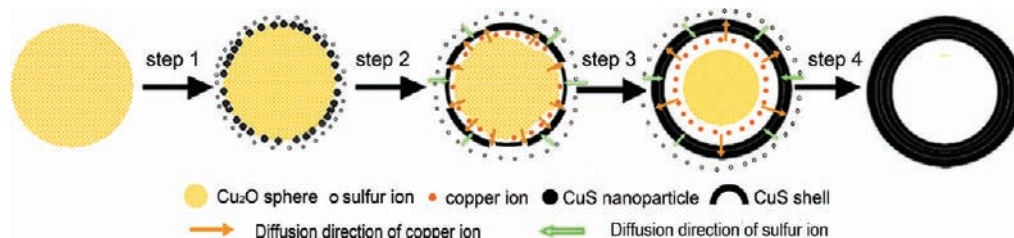


**Figure 7.** Schematic illustration of growth mechanism of CuS hollow spheres.

faster than that on the inside of the shell. The consumption rate of the  $\text{Cu}_2\text{O}$  core is larger than the production rate of  $\text{CuS}$  on the inside of the shell. As a result, the outer diameter of the formed  $\text{CuS}$  shell is larger than that of the precursor  $\text{Cu}_2\text{O}$  spheres, while the inner diameter becomes smaller. At the same time, a gap between the  $\text{Cu}_2\text{O}$  core and the  $\text{CuS}$  shell is formed. While the reaction goes on, the  $\text{Cu}_2\text{O}/\text{CuS}$  core/shell structures completely transform to  $\text{CuS}$  hollow spheres through the Kirkendall effect, which is similar to the synthesis of  $\text{CoS}$ ,  $\text{ZnO}$  hollow spheres and  $\text{Cu}_7\text{S}_4$  hollow polyhedron, and so on.<sup>11,15,16</sup> In the synthesis, the diffusion across the sphere's shell is the slowest process, determining the whole synthesis velocity. Increase the diffusion velocity or/and decrease the amount of effective material of every core that is to be completely removed through diffusion and the hollow structure will be synthesized even faster. In the reported synthesis of hollow structures by the Kirkendall effect, most of the core templates were single crystal or solid polycrystal aggregates.<sup>11,15–25</sup> The amount of core materials that must be completely removed through diffusion was large, so a high reaction temperature or/and a long time were thus needed, especially in the case of large-sized templates. In this work, the fast formation of  $\text{CuS}$  hollow spheres can be attributed to three factors: (1) the  $\text{Cu}_2\text{O}$  spheres are composed of nanoparticles. The nanoparticles have very high reactivity, even at low temperature; (2) the  $\text{Cu}_2\text{O}$  spheres are loose aggregates of nanoparticles, which means that the amount of core materials that have to be consumed is less. As a result, the required time to completely consume the core is shorter. (3) the produced  $\text{CuS}$  shell is of a polycrystalline structure, which is in favor of the mass diffusion and transference through the grain boundary. This work provides new insights into the fast preparation of other hollow microspheres under mild conditions.

**3.4. Control of the Thickness of Hollow Spheres.** In this method, the shell thickness of the hollow spheres is mainly determined by the amount of effective reactants supplied by the core templates. Therefore, it is expected that the shell thickness can be controlled by adjusting the aggregation degree of  $\text{Cu}_2\text{O}$  nanoparticles. Figure 8a is the TEM image of  $\text{Cu}_2\text{O}$  spheres obtained by increasing the amount of PVP to 0.48 g (other experimental parameters were not changed). The aggregates of these  $\text{Cu}_2\text{O}$  spheres are much looser (compared with Figure 2b). Using them as core templates, the obtained  $\text{CuS}$  are hollow spheres with shell thickness of about 20 nm (Figure 8c). Decreasing the PVP amount to 0.15 g and increasing the pH value of  $\text{NaOH}$  solution to 10, the obtained  $\text{Cu}_2\text{O}$  spherical aggregates are more compacted (compared with Figure 2b). Using them as core templates, the obtained  $\text{CuS}$  hollow spheres have a shell thickness of about 50–60 nm (Figure 8d). The above experimental results show that the shell thickness of the hollow sphere can be controlled

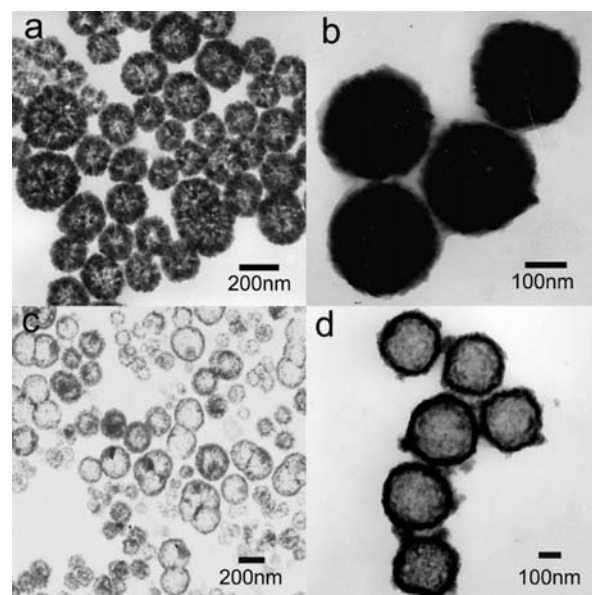


**Figure 8.** TEM images of  $\text{Cu}_2\text{O}$  templates (a, b) and corresponding  $\text{CuS}$  hollow spheres (c, d), respectively. The  $\text{Cu}_2\text{O}$  sample in (a) was obtained with PVP of 0.48 g. The  $\text{Cu}_2\text{O}$  sample in (b) was obtained with PVP of 0.15 g and a pH value of 10.

easily by adjusting the aggregation degree of the  $\text{Cu}_2\text{O}$  nanoparticles.

#### 4. Conclusions

A rapid and mild solution method for the preparation of  $\text{CuS}$  hollow spheres has been realized by using spherical aggregates of  $\text{Cu}_2\text{O}$  nanoparticles as sacrificial templates. The results show that the formation of loose aggregates of  $\text{Cu}_2\text{O}$  nanoparticles is the key to the fast synthesis of hollow spheres at low temperature. The shell thickness of hollow spheres can be controlled easily by adjusting the aggregation degree of  $\text{Cu}_2\text{O}$  nanoparticles. This method could be extended to the fast and mild synthesis of other hollow structures with controllable shell thickness.

**Acknowledgment.** This work was supported by the National Natural Science Foundation of China (50872061), the Foundation of Fuzhou University State Key Laboratory Breeding Base of Photocatalysis (K-081030), and the Foundation of Qingdao Science and Technology (07-2-3-12-jch). The authors thank the four reviewers for their valuable advice to improve the quality of this article.

**Supporting Information Available:** Detailed characterization, including XPS spectra of  $\text{Cu}_2\text{O}$  spheres (Figure S1) and  $\text{CuS}$  hollow spheres (Figure S2), TG curve (Figure S3) and PL spectrum (Figure S4) of  $\text{CuS}$  hollow spheres. This material is available free of charge via the Internet at <http://pubs.acs.org>.